Higgs potential and hidden light Higgs scenario in two Higgs doublet models

Sanghyeon Chang,[1] Sin Kyu Kang,[2] Jong-Phil Lee,[3] and Jeonghyeon Song[4]

[1]*Center for Theoretical Physics of the Universe, IBS, Daejeon 305-811, Korea*
[2]*School of Liberal Arts, Seoul-Tech, Seoul 139-743, Korea*
[3]*School of Electrical Engineering and BK21 Plus Humanware Information Technology,*
Korea University, Seoul 136-713, Korea
[4]*School of Physics, Konkuk University, Seoul 143-701, Korea*

In two Higgs doublet models, there exists an interesting possibility, the hidden light Higgs scenario, that the discovered SM-like Higgs boson is the heavier CP-even Higgs boson H^0 and the lighter CP-even h^0 has not been observed yet in any experiment. We study the current status of this scenario in Types I, II, X, and Y, through the scans of the parameters with all relevant theoretical and experimental constraints. We employ not only the most up-to-date Higgs signal strength measurements with the feed-down effects, but also all the available LHC exclusion limits from heavy Higgs searches. Adjusting the heavier H^0 to the 125 GeV state while hiding the lighter h^0 from the LEP Higgs search prohibits the extreme decoupling limit: there exist upper bounds on the masses of the pseudoscalar A^0 and the charged Higgs $H^\pm$ below about 600 GeV. In addition, the Z_2 symmetry is shown to be a good approximate symmetry since the soft Z_2 symmetry breaking parameter m_{12}^2 should be less than about $(45\text{ GeV})^2$. Most interestingly, a few parameters in the Higgs potential and the related Higgs triple and quartic couplings are shown to be meaningfully constrained by the current data. The double Higgs-strahlung process at an e^+e^- collider is also studied.

I. INTRODUCTION

The observation of a Higgs boson with mass around 125 GeV at the LHC [1] completes the journey in the standard model (SM): the electroweak symmetry breaking mechanism is uncovered; the mass generation of subatomic particles is most economically explained; the Higgs boson mass, the last unknown parameter in the SM, is precisely measured [2]. The current LHC Higgs data imply that the observed 125 GeV state h_{125} is very similar to the SM Higgs boson [3–7]. Nevertheless there are some vital clues that this is not the end of the road. We do not expect that the ultimate theory of particle physics is the SM which suffers from the gauge hierarchy problem and has no solution to account for 95% of the energy of the Universe. New physics is inevitable.

Apart from Occam's Razor, there is no reason for prohibiting additional Higgs doublets. Many new physics models contain at least two Higgs doublets, and thus additional Higgs bosons. This extension of the Higgs sector is a good direction toward new physics beyond the SM. The LHC Higgs data on the 125 GeV state may play the role of a compass to show the direction. In addition, both ATLAS and CMS collaborations provide significant exclusion limits from the null results in the searches for the heavy neutral and charged Higgs bosons. In the ordinary setup where the observed is the lightest CP-even neutral Higgs boson h^0, the compass naturally points to the decoupling limit [8] where the other Higgs states are

very heavy. The phenomenology of the decoupling limit generically mimics that of the SM. Even if the current experimental status, the SM-like 125 GeV state without any signal of other Higgs bosons, might keep in the future, the verification or invalidation of a specific new physics model will be postponed till the next generation collider.

If the observed 125 GeV state is a *heavier CP*-even neutral Higgs boson H^0, however, the LHC Higgs data play a much more significant role in characterizing a specific model. Adjusting the heavier H^0 to h_{125} as well as hiding the lighter h^0 from low energy experiment data constrain the new physics model strongly. We call this possibility the *hidden light Higgs scenario*. If the current LHC data can specify the Higgs potential in this scenario thanks to the expected strong constraints, it will give important implications on the dynamics of the electroweak phase transition [9,10], and the measurement of the cubic and quartic self-couplings of Higgs bosons in the future collider [11,12].

As the simplest extension of the SM Higgs sector, we consider a two Higgs doublet model (2HDM) [13] with CP invariance and softly broken Z_2 symmetry [14]. There exist five physical Higgs bosons, the light CP-even scalar h^0, the heavy CP-even scalar H^0, the CP-odd pseudoscalar A^0, and two charged Higgs bosons $H^\pm$. The general Higgs potential has 7 parameters. According to the Z_2 charges of the SM quarks and leptons, there exist four types of 2HDM: Type I, Type II, Type X, and Type Y [15,16]. In the normal setup of $h^0 = h_{125}$, there are extensive studies on the global fit

analysis of the Higgs signal strengths as well as the phenomenology of the other heavy Higgs bosons [17–28]. The hidden light Higgs scenario is also naturally accommodated in the 2HDM [6,29–35]: H^0 is the 125 GeV state and h^0 has not been observed yet.

A comprehensive study of the current status of the 2HDM Type I and Type II by including the heavy Higgs search data was first performed in Ref. [36]. Similar comprehensive studies in other setups such as very light Higgs bosons [31] or the minimal supersymmetric standard model [37] were followed up. We extend the study, focusing on the question of how much the current data constrain the Higgs *potential* in the hidden light Higgs scenario. To answer the question, we consider more extended constraints than in Ref. [36], particularly those from the LHC heavy Higgs searches. We classify the theoretical and phenomenological constraints into three categories: theoretical bounds, pre-LHC bounds, and LHC bounds.

The details of each step are summarized in Table I. The theoretical bounds demand the boundedness of the Higgs potential [38], unitarity [39,40], and perturbativity. The "pre-LHC" bounds include the LEP bounds on h^0 [41,42] and $H^\pm$ [43], $\Delta\rho$ in the electroweak precision data [44,45], the flavor changing neutral current (FCNC) data such as ΔM_{B_d} and $b \to s\gamma$ [46,47], and the top quark decay of $t \to H^+ b$ [48]. The "LHC" bounds are based not only on the Higgs signal strength measurements from LHC8, but also on the exclusion limits from all the heavy Higgs searches including $H^\pm \to \tau^\pm \nu_\tau$ [49,50], $H^+ \to c\bar{s}$ [51], $gg \to A^0 \to \gamma\gamma$ [52,53], $gg \to A^0 \to \tau^+\tau^-$ [54,55], and $b\bar{b} \to A^0 \to \tau^+\tau^-$ [54,55]. For the 125 GeV state data, we perform the comprehensive global χ^2 analysis by including $H^0 \to h^0 h^0$ and $H^0 \to A^0 A^0$ as well as "feed-down" (FD) contributions from the production of heavier Higgs bosons through their decay into H^0 [36,56], not by just limiting the FD signal strength value.

We shall show that in all four types, the hidden light Higgs scenario is consistent with the data, as good as the SM. In addition, the survived parameter points have many interesting implications. Major ones are as follows: (i) there exist *upper* bounds on the heavy Higgs bosons like $m_{A,H^\pm} \lesssim 600$ GeV; (ii) the soft Z_2 symmetry breaking term m_{12}^2 is strongly constrained to be below about $(45 \text{ GeV})^2$ in most cases; (iii) in Type I and X, a light m_A (as low as 20 GeV) and $m_{H^\pm}$ (as low as 100 GeV) are allowed; (iv) the triple Higgs coupling g_{HHH} is very like the SM Higgs triple coupling, and g_{hHH} is similar to the SM value; (v) the quartic Higgs couplings g_{HHHH} and g_{hHHH} are similar to the SM value. Inspired by the almost fixed g_{HHH} and g_{hHH}, we study the double Higgs-strahlung at an e^+e^- collider, $e^+e^- \to Z^0 H^0 H^0$, which can be highly enhanced in some parameter space where the resonance production of A^0 is allowed. These are our main results.

The paper is organized as follows. In Sec. II, we briefly review the 2HDM. Section III summarizes the constraints. Section IV presents our results, the allowed parameter space stage by stage. In Sec. V, we show the Higgs triple and quartic couplings in the allowed parameter space, and study the future prospect of $e^+e^- \to Z^0 H^0 H^0$. Section VI contains our conclusions.

II. BRIEF REVIEW OF THE 2HDM

A 2HDM [13] introduces two complex $SU(2)_L$ Higgs doublet scalar fields, Φ_1 and Φ_2. Both Φ_1 and Φ_2 develop nonzero vacuum expectation values as $\langle \Phi_{1,2} \rangle = (0, v_{1,2}/\sqrt{2})^T$, which generate the electroweak symmetry breaking. When parametrizing $t_\beta = v_2/v_1$, one linear combination $H_1 = c_\beta \Phi_1 + s_\beta \Phi_2$ has nonzero vacuum expectation value of $v = \sqrt{v_1^2 + v_2^2} = 246$ GeV, while its orthogonal combination $H_2 = -s_\beta \Phi_1 + c_\beta \Phi_2$ acquires zero vacuum expectation value. For simplicity of notation, we take $s_x = \sin x$, $c_x = \cos x$, and $t_x = \tan x$. We define the fluctuation fields about the minima v_1 and v_2 as

$$\Phi_i = \begin{pmatrix} \phi_i^+ \\ \frac{v_i + \rho_i + i\eta_i}{\sqrt{2}} \end{pmatrix}, \qquad i = 1, 2. \tag{1}$$

In order to avoid FCNC at the lowest order, a discrete Z_2 symmetry is imposed, under which $\Phi_1 \to \Phi_1$ and $\Phi_2 \to -\Phi_2$ [14].

The most general potential with CP invariance and softly broken Z_2 symmetry is

$$V = m_{11}^2 \Phi_1^\dagger \Phi_1 + m_{22}^2 \Phi_2^\dagger \Phi_2 - m_{12}^2 (\Phi_1^\dagger \Phi_2 + \text{H.c.})$$
$$+ \frac{1}{2}\lambda_1 (\Phi_1^\dagger \Phi_1)^2 + \frac{1}{2}\lambda_2 (\Phi_2^\dagger \Phi_2)^2 + \lambda_3 (\Phi_1^\dagger \Phi_1)(\Phi_2^\dagger \Phi_2)$$
$$+ \lambda_4 (\Phi_1^\dagger \Phi_2)(\Phi_2^\dagger \Phi_1) + \frac{1}{2}\lambda_5 [(\Phi_1^\dagger \Phi_2)^2 + \text{H.c.}]. \tag{2}$$

The CP invariance requires all of the parameters to be real, and m_{12}^2 breaks the Z_2 symmetry softly. Note that the m_{12}^2 parameter can be negative. Using the tadpole condition, m_{11} and m_{22} can be written in terms of v, t_β, and $\lambda_{1,...,5}$. The Higgs potential has 7 free parameters of m_{12}^2, t_β, and $\lambda_{1,...,5}$.

The charged Higgs boson $H^\pm$ is a linear combination of $\phi_1^\pm$ and $\phi_2^\pm$, and the pseudoscalar A^0 is a linear combination of η_1 and η_2. Their orthogonal states are Goldstone modes $G^\pm$ and G^0, respectively. And their masses are

$$m_{H^\pm}^2 = \frac{m_{12}^2}{c_\beta s_\beta} - (\lambda_4 + \lambda_5)v^2, \qquad m_A^2 = \frac{m_{12}^2}{c_\beta s_\beta} - 2\lambda_5 v^2. \tag{3}$$

The physical CP-even Higgs bosons h^0 and H^0 are obtained through the diagonalization of the mass squared matrix $\mathcal{M}_0^2$ with the mixing angle α, given by

TABLE I. Summary of constraints.

Theoretical stability (yellow)	i V_H to be bounded below ii Unitarity iii Perturbativity of quartic couplings
Pre-LHC bounds (green)	iv LEP bounds on h^0 and $H^\pm$ v $\Delta\rho$ in the electroweak precision data vi FCNC like ΔM_{B_d} and $b \to s\gamma$ vii Top quark decay into $H^\pm$

LHC bounds (red)	viii $m_H = 125$ GeV
	ix LHC search for $H^\pm$ via $pp \to t\bar{t}H^\pm$ followed by $H^\pm \to \tau\nu$
	x LHC search for A^0 via $gg \to A^0 \to \gamma\gamma, \tau^+\tau^-$ and $b\bar{b} \to A^0 \to \tau^+\tau^-$
	xi Global χ^2 fit to the LHC Higgs data including
	  (a) Additional decay channels of $H^0 \to h^0 h^0$, $A^0 A^0$, $H^+ H^-$, $W^\pm H^\mp$
	  (b) the "feed-down"

$$\mathcal{M}_0^2 = \begin{pmatrix} \mathcal{M}_{11}^2 & \mathcal{M}_{12}^2 \\ \mathcal{M}_{12}^2 & \mathcal{M}_{22}^2 \end{pmatrix} \qquad (4)$$

where

$$\mathcal{M}_{11}^2 = m_{12}^2 t_\beta^2 + \frac{\lambda_1 v^2}{1 + t_\beta^2}, \qquad \mathcal{M}_{22}^2 = \frac{m_{12}^2}{t_\beta^2} + \lambda_2 v^2 \frac{t_\beta^2}{1 + t_\beta^2}$$

$$\mathcal{M}_{12}^2 = -m_{12}^2 + \lambda_{345} v^2 \frac{t_\beta}{1 + t_\beta^2}, \qquad (5)$$

where $\lambda_{345} = \lambda_3 + \lambda_4 + \lambda_5$. The masses of neutral Higgs m_h and m_H are

$$m_{H,h}^2 = \frac{1}{2}\left[\mathcal{M}_{11}^2 + \mathcal{M}_{22}^2 \pm \sqrt{(\mathcal{M}_{11}^2 - \mathcal{M}_{22}^2)^2 + 4(\mathcal{M}_{12}^2)^2}\right]. \qquad (6)$$

The SM Higgs field, which corresponds to H_1, becomes

$$h_{\mathrm{SM}} = s_{\beta-\alpha} h^0 + c_{\beta-\alpha} H^0. \qquad (7)$$

If $c_{\beta-\alpha} = 1$ and $m_H = 125$ GeV, H^0 has the same properties as the SM Higgs boson. This is called the alignment limit [57]:

The alignment limit for $H^0 = h_{\mathrm{SM}}$: $c_{\beta-\alpha} = 1$. (8)

As shall be shown, the allowed parameters by all the constraints are distributed around the alignment limit. The alignment limit maximizes or minimizes some triple couplings of Higgs bosons with weak gauge bosons or other Higgs bosons. We classify them into two categories, one proportional to $s_{\beta-\alpha}$ and the other proportional to $c_{\beta-\alpha}$:

$$s_{\beta-\alpha}: g_{hW^+W^-}, \quad g_{hZZ}, \quad g_{ZAH}, \quad g_{W^\pm H^\mp H},$$
$$c_{\beta-\alpha}: g_{HW^+W^-}, \quad g_{HZZ}, \quad g_{ZAh}, \quad g_{W^\pm H^\mp h}, \quad g_{Hhh}. \qquad (9)$$

In the hidden light Higgs scenario, the couplings proportional to $s_{\beta-\alpha}$ vanish in the alignment limit.

Yukawa couplings of Higgs bosons are different according to the 2HDM type. Focusing on the 125 GeV state H^0, we present the normalized Yukawa couplings by the SM values, $\hat{y}_{uu,dd,\ell\ell}^H$, in terms of $c_{\beta-\alpha}$ and $s_{\beta-\alpha}$:

	$c_{\beta-\alpha} - \frac{s_{\beta-\alpha}}{t_\beta}$	$c_{\beta-\alpha} + t_\beta s_{\beta-\alpha}$
Type I	$\hat{y}_{uu}^H, \hat{y}_{dd}^H, \hat{y}_{\ell\ell}^H$	
Type II	$\hat{y}_{uu}^H$	$\hat{y}_{dd}^H, \hat{y}_{\ell\ell}^H$
Type X	$\hat{y}_{uu}^H, \hat{y}_{dd}^H$	$\hat{y}_{\ell\ell}^H$
Type Y	$\hat{y}_{uu}^H, \hat{y}_{\ell\ell}^H$	$\hat{y}_{dd}^H$

(10)

Note that in the exact alignment limit ($c_{\beta-\alpha} = 1$), all of the Yukawa couplings for H^0 are the same as in the SM. There are two kinds of deviation from the alignment limit: one is proportional to t_β, and the other to $1/t_\beta$. Since FCNC constrains $t_\beta \gtrsim 1$, those proportional to $t_\beta s_{\beta-\alpha}$ yield much larger deviation from the SM Yukawa coupling. As shown in Eq. (10), Type I has common Yukawa couplings, which have the t_β-suppressed deviation from the alignment. On the while, Type II has the t_β-enhanced deviation for the down-type quark and charged lepton Yukawa couplings. As shall be shown later, Type II is most strongly constrained by the current LHC Higgs data.

III. CONSTRAINTS

We constrain the hidden light Higgs scenario in the 2HDM by sequentially taking three steps. The first step (yellow) is to apply theoretical conditions, the second (green) is to use all reliable experimental constraints before the LHC data, and the last step (red) is to include the LHC Higgs data that consist of the observation of the 125 GeV state as well as the exclusion limits from the searches for the other Higgs bosons heavier than 125 GeV. In what follows, each colored point (yellow, green, or red)

represents the surviving parameters at 95% C.L., up to the corresponding step. For example, the green points satisfy the theoretical and pre-LHC bounds. We summarize the constraints in Table I.

A. Theoretical constraints

(i) *The Higgs potential to be bounded from below*: As proven in Ref. [38], the scalar potential in Eq. (2) is bounded from below if and only if the following conditions are satisfied:

$$\lambda_1 > 0, \qquad \lambda_2 > 0, \qquad \lambda_3 > -\sqrt{\lambda_1\lambda_2},$$
$$\lambda_3 + \lambda_4 - |\lambda_5| > -\sqrt{\lambda_1\lambda_2}. \tag{11}$$

(ii) *Unitarity*: Tree level perturbative unitarity requires for the absolute values of the followings to be less than 8π [39,40]:

$$a_\pm = \frac{3}{2}(\lambda_1 + \lambda_2) \pm \sqrt{\frac{9}{4}(\lambda_1 - \lambda_2)^2 + (2\lambda_3 + \lambda_4)^2},$$
$$b_\pm = \frac{1}{2}(\lambda_1 + \lambda_2 \pm \sqrt{(\lambda_1 - \lambda_2)^2 + 4\lambda_4^2}),$$
$$c_\pm = \frac{1}{2}(\lambda_1 + \lambda_2 \pm \sqrt{(\lambda_1 - \lambda_2)^2 + 4\lambda_5^2}),$$
$$f_+ = \lambda_3 + 2\lambda_4 + 3\lambda_5, \quad f_- = \lambda_3 + \lambda_5, \quad f_1 = \lambda_3 + \lambda_4,$$
$$e_1 = \lambda_3 + 2\lambda_4 - 3\lambda_5, \quad e_2 = \lambda_3 - \lambda_5, \quad p_1 = \lambda_3 - \lambda_4. \tag{12}$$

(iii) *Perturbativity*: We first demand the bare quartic couplings in the Higgs potential to satisfy the perturbativity as

$$|\lambda_i| < 4\pi, \qquad i = 1, \dots, 5. \tag{13}$$

In addition, the magnitudes of the quartic couplings among physical Higgs states like $g_{\varphi_i\varphi_j\varphi_k\varphi_\ell}(\phi_i = h^0, H^0, A^0, H^\pm)$ are required to be smaller than 4π.

Here we do not require that the 2HDM vacuum should be the global minimum of the potential [58], because the existence of a false vacuum (local minimum) is acceptable if its lifetime is longer than the age of the Universe. Unquestionably if the lifetime of a false vacuum is shorter, the corresponding parameter space should be excluded. Since the calculation of the 2HDM vacuum lifetime is beyond the scope of this study, we take a conservative stance to ignore the global minimum condition.

B. pre-LHC bounds

(i) *The LEP bounds on h^0 and $H^\pm$*: One of the most direct channels to probe a light Higgs boson with

mass below 120 GeV is the Higgs-strahlung at the LEP. We use the strongest upper bound on the event rate of $e^+e^- \to Z^0 h^0 \to Z^0 jj$ [41,42]. Another important result from the LEP is the direct production limit on the charged Higgs boson mass as [43]:

$$m_{H^\pm} \geq 80 \text{ GeV}. \tag{14}$$

(ii) *$\Delta\rho$ in the electroweak precision data*: The $\Delta\rho$ parameter from the electroweak precision measurement has additional contributions in the 2HDM through the heavy neutral Higgs bosons (A^0 in the hidden light Higgs scenario) as well as the charged Higgs bosons [44,45]. With the observed Higgs boson mass, its global fit result has been improved significantly as [43]

$$\Delta\rho = 0.00040 \pm 0.00024. \tag{15}$$

It is known that the new contribution is suppressed if $m_A \simeq m_{H^\pm}$ or $m_H \simeq m_{H^\pm}$ [59,60]. As shall be discussed, the $m_H \simeq m_{H^\pm} \simeq 125$ GeV case is prohibited by the FCNC constraints in Types II and Y.

(iii) *FCNC processes such as ΔM_{B_d} and $b \to s\gamma$*: In the 2HDM, the charged Higgs boson contributes to various FCNC processes through the loop. We consider two sensitive FCNC processes, $b \to s\gamma$ [46,47] and ΔM_{B_d} [47,61]. ΔM_{B_d} excludes small t_β region for all types, while $b \to s\gamma$ further excludes the light charged Higgs mass region in Type II and Type Y. Other processes such as ε_K [62] and R_b [63,64] impose weaker constraints [65]. We do not consider the measurements of $R(D^{(*)}) \equiv \text{Br}(\bar{B} \to D^{(*)}\tau^-\bar{\nu}_\tau)/\text{Br}(\bar{B} \to D^{(*)}l^-\bar{\nu}_l)$ from *BABAR* [66].[1]

(iv) *Bound from $t \to bH^+$*: A light charged Higgs boson could have appeared in the top decay into bH^+ if kinematically allowed. We include the Tevatron search results of the upper bounds on $\text{Br}(t \to bH^+)$ [48].

C. LHC bounds

(i) *Higgs mass bounds*: Both ATLAS and CMS collaborations measured the Higgs boson mass with high precision [69,70]. The combined result is [71]

$$m_H = 125.09 \pm 0.21(\text{stat}) \pm 0.11(\text{syst}) \text{ GeV}. \tag{16}$$

We demand that m_H be within 2σ. In addition, we exclude the degenerate cases of $m_H = m_A$ and

---

[1]Recently, LHCb [67] reported 2.1σ excess of $R(D^*)$ over the SM predictions, and Belle [68] presented a new measurements of $R(D)$ and $R(D^*)$ which are not significantly deviated from both the SM prediction and the measured values at *BABAR* [66] and LHCb.

TABLE II. Summary of the LHC Higgs signal strengths at 7 and 8 TeV.

Production	ATLAS	CMS
ggF + $t\bar{t}h$	$\tilde{R}^{gg\mathrm{F}}_{\gamma\gamma} = 1.32 \pm 0.38$ [3], $\tilde{R}^{t\bar{t}h}_{\gamma\gamma} = 1.3^{+2.6}_{-1.7}$ [4] $\tilde{R}^{gg\mathrm{F}}_{WW} = 1.01^{+0.27}_{-0.20}$ [77] $\tilde{R}^{gg\mathrm{F}+t\bar{t}h}_{ZZ} = 1.52^{+0.85}_{-0.65}$ [78] $\tilde{R}^{gg\mathrm{F}}_{\tau\tau} = 1.93^{+1.45}_{-1.15}$ [79] $\tilde{R}^{t\bar{t}h}_{b\bar{b}} = 1.7 \pm 1.4$ [80,81]	$\tilde{R}^{gg\mathrm{F}+t\bar{t}h}_{\gamma\gamma} = 1.13^{+0.37}_{-0.31}$ [5] $\tilde{R}^{gg\mathrm{F}}_{WW} = 0.74^{+0.22}_{-0.20}$ [82] $\tilde{R}^{gg\mathrm{F}+t\bar{t}h}_{ZZ} = 0.80^{+0.46}_{-0.36}$ [83] $\tilde{R}^{gg\mathrm{F}}_{\tau\tau} = 0.93 \pm 0.42$ [84] $\tilde{R}^{t\bar{t}h}_{b\bar{b}} = 0.67^{+1.35}_{-1.33}$ [85]
VBF + Vh	$\tilde{R}^{\mathrm{VBF}}_{\gamma\gamma} = 0.8 \pm 0.7,$ $\tilde{R}^{WH}_{\gamma\gamma} = 1.0 \pm 1.6$, $\tilde{R}^{ZH}_{\gamma\gamma} = 0.1^{+3.7}_{-0.1}$ [3] $\tilde{R}^{\mathrm{VBF}}_{WW} = 1.28^{+0.53}_{-0.45}$ [77] $\tilde{R}^{\mathrm{VBF}+Vh}_{ZZ} = 0.90^{+4.5}_{-2.0}$ [78] $\tilde{R}^{\mathrm{VBF}+Vh}_{\tau\tau} = 1.24^{+0.58}_{-0.54}$ [79] $\tilde{R}^{Vh}_{b\bar{b}} = 0.51^{+0.40}_{-0.37}$ [86]	$\tilde{R}^{\mathrm{VBF}+Vh}_{\gamma\gamma} = 1.15^{+0.63}_{-0.58}$ [5] $\tilde{R}^{\mathrm{VBF}}_{WW} = 0.60^{+0.57}_{-0.46}$, $\tilde{R}^{Vh}_{WW} = 0.39^{+1.97}_{-1.87}$ [82] $\tilde{R}^{\mathrm{VBF}+Vh}_{ZZ} = 1.7^{+2.2}_{-2.1}$ [83] $\tilde{R}^{\mathrm{VBF}}_{\tau\tau} = 0.94 \pm 0.41,$ $\tilde{R}^{Vh}_{\tau\tau} = -0.33 \pm 1.02$ [84] $\tilde{R}^{\mathrm{VBF}}_{b\bar{b}} = 0.7 \pm 1.4$ [85], $\tilde{R}^{Vh}_{b\bar{b}} = 1.0 \pm 0.5$ [87]

$m_h = m_H$ in order to avoid the possible contributions from h^0 or A^0 to the observed Higgs signal strengths. Both m_h and m_A should lie outside m_H at 2σ.

(ii) *LHC search for the charged Higgs boson*: The search strategy of the charged Higgs boson at the LHC is different according to its mass. For $m_{H^\pm} > m_t + m_b$, the main decay mode is into $t\bar{b}$ [72]. For lighter charged Higgs boson than the top quark, two decay channels are searched, $H^\pm \to \tau^\pm \nu_\tau$ [49,50] and $H^+ \to c\bar{s}$ [51]. Since the direct production of the charged Higgs boson is very small, the bound for the charged Higgs boson is weak in general. The strongest bound is from $pp \to t\bar{t} \to b\bar{b}H^\pm W^\mp$, followed by $H^\pm \to \tau^\pm \nu$. We include the upper bounds on $\mathrm{Br}(t \to H^+ b) \times \mathrm{Br}(H^+ \to \tau^+ \nu_\tau)$.

(iii) *LHC search for A^0*: In the hidden light Higgs scenario, only A^0 is the heavy neutral Higgs boson. Up to now, there are no significant excesses in the heavy neutral Higgs search, which provides the exclusion limit. We include the $gg \to A^0 \to \gamma\gamma$ [52,53], $gg \to A^0 \to \tau^+\tau^-$ [54,55], and $b\bar{b} \to A^0 \to \tau^+\tau^-$ [54,55]. Note that the W^+W^- and Z^0Z^0 decay channels are not relevant for the pseudoscalar A^0. Another important decay channel is into $t\bar{t}$, which is dominant if $m_A > 2m_t$ and $t_\beta \lesssim 10$ [60]. Although both ATLAS and CMS collaborations reported the $t\bar{t}$ resonance search results [73], the interpretation is very challenging at a hadron collider because the interference with the QCD continuum background causes various shapes in the $t\bar{t}$ invariant mass distribution [74–76]. Since the interference effects have not been included yet in the experiment analysis, we do not consider this $t\bar{t}$ channel.

(iv) *the global fit to the LHC 125 GeV state data with the FD effects*: The discovery of the Higgs boson is not based on a single observation of a resonance, but more than 200 channels. Any new physics model should explain the whole LHC Higgs data, which is commonly analyzed through the global χ^2 fit. We parametrize each signal rate by $R^{\mathrm{prduction}}_{\mathrm{decay}}$, the ratio of the observed event rate to the SM expectation in the specific channel, and identify it with the signal strength modifier $\mu \equiv \sigma/\sigma_{\mathrm{SM}}$. In the 2HDM, R's are not generally equal to one as in the SM. The latest experimental values, denoted by $\tilde{R}$'s, are summarized in Table II. We perform global χ^2 fits of 7 model parameters to the observed Higgs signal strength $\tilde{R}_i$.

In the 2HDM, there are three sources to deviate the signal strength value from one. First, the effective couplings of H^0 with the SM particles can be different from those in the SM, which happens when $c_{\beta-\alpha} \neq 1$. Second, there are additional decay channels of H^0 into h^0h^0, A^0A^0, Z^0A^0, $W^\pm H^\mp$, and H^+H^-. Too large decay rates of new decay modes enhance the total decay rate of H^0, which affects the observed signal strengths. We include these decay rates to the global χ^2 fit. In the hidden light Higgs scenario, the $H^0 \to h^0h^0$ mode excludes considerable parameter space even in the alignment limit, since the vertex is proportional to $c_{\beta-\alpha}$. On the contrary, the vertices of Z^0-A^0-H^0 and $W^\pm$-$H^\mp$-H^0 are proportional to $s_{\beta-\alpha}$, and thus $H^0 \to Z^0A^0$, $W^\pm H^\mp$ are suppressed in the alignment limit: see Eq. (9). The LEP bounds of $m_{H^\pm} \geq 80$ GeV kinematically suppresses $H^0 \to H^+H^-$.

The third source for the deviation is the FD effects [36,56]: the inclusive decay of heavy Higgs states

into H^0 yields more events in the 125 GeV state, which renders the H^0 not to be SM-like even in the alignment limit. In the hidden light Higgs scenario, dominant contribution to the FD effects is from the inclusive decay of A^0 into H^0. The $H^\pm$ contribution is negligible since its production at the LHC is too small. The general probability of the inclusive production of H^0 from A^0 decay is [36]

$$\mathcal{P}_{\text{FD}}(A^0 \to H^0 + X) = 2\text{Br}(A^0 \to H^+H^-)\text{Br}(H^+ \to W^+H^0)^2 + \text{Br}(A^0 \to Z^0H^0)$$
$$+ 2\text{Br}(A^0 \to W^-H^+)\text{Br}(H^+ \to W^+H^0)$$
$$+ 2\text{Br}(A^0 \to H^+H^-)\text{Br}(H^+ \to W^+H^0)\{1 - \text{Br}(H^+ \to W^+H^0)\}. \quad (17)$$

As shall be shown in the next section, the "pre-LHC" constraints allow two kinds of regions in the $(m_{H^\pm}, m_A)$ parameter space. One is $m_{H^\pm} \simeq m_A$ in all four types, and the other allows $m_{H^\pm} \approx 100$ GeV. Only the $\text{Br}(A^0 \to Z^0H^0)$ in Eq. (17) is kinematically relevant.

We define new FD signal strengths as

$$\mu_{ii}^{\text{FD:ZH}} = \frac{\sigma(pp \to gg \to A^0)\text{Br}(A^0 \to Z^0H^0)}{\sigma(pp \to Z^0h_{\text{SM}})}$$
$$\times \frac{\text{Br}(H^0 \to ii)}{\text{Br}(h_{\text{SM}} \to ii)}, \quad (18)$$

where $i = \gamma$, W, Z, τ, b.[2] We add $\mu_{ii}^{\text{FD:ZH}}$ to R_{ii}^{ZH} and perform the global χ^2 fit to the observed $\tilde{R}$'s.

IV. RESULTS

For the 7 parameters of $\lambda_{1,...,5}$, t_β, and m_{12}^2, we randomly generate 2×10^{10} points to scan over the following ranges:

$$\lambda_{1,2} \in [0, 4\pi], \qquad \lambda_{3,4,5} \in [-4\pi, 4\pi],$$
$$t_\beta \in [1, 50], \qquad m_{12}^2 \in [-(2 \text{ TeV})^2, (2 \text{ TeV})^2]. \quad (19)$$

We apply three steps of bounds:
Step-1 (yellow) theoretical bounds;
Step-2 (green) the pre-LHC bounds;
Step-3 (red) the LHC bounds.
The detailed conditions are summarized in Table I. In what follows, yellow, green, and red points denote the survived parameters after Step-1, Step-2, and Step-3 bounds, respectively. Note that the bound conditions are accumulatively applied. The red points satisfy all the bounds.

(i) *High reliability of the hidden light Higgs scenario*: We find that the hidden light Higgs scenario is consistent with all the current data. Out of 2×10^{10} parameter sets and at 95% C.L., 2.2×10^4 points survived in Type I, 0.74×10^4 in Type II, 1.1×10^4 in Type X, and 1.4×10^4 in Type Y. Limited but substantial parameter space is consistent with the current data. Type I has the largest allowed parameter space while Type II has the smallest. The minimum values of χ^2 per degree of freedom are 0.40, 0.51, 0.51, 0.50 in Type I, II, X, and Y, respectively. In the SM, it is 0.49. The best fit points in the 2HDM explain the current data at least as good as the SM.

(ii) *Upper bounds on m_A and $m_{H^\pm}$*: A unique feature of the hidden light Higgs scenario is the presence of the upper bounds on heavy Higgs boson masses, m_A and $m_{H^\pm}$. In the normal setup where $h_{125} = h^0$, the so-called decoupling limit can be always taken such that all of the new particles are heavy enough to be beyond the LHC reach. A safety zone for avoiding the invalidation of the model by the experimental data is guaranteed. In the hidden light Higgs scenario, however, matching the heavy H^0 to the 125 GeV state constrains the other heavy Higgs bosons, A^0 and $H^\pm$.

Figure 1 presents the allowed m_A and $m_{H^\pm}$ in Type I and Type II. The results for Type X (Type Y) are very similar to Type I (Type II). As summarized in Table I, yellow, green, and red points satisfy theoretical bounds, pre-LHC constraints, and LHC constraints, respectively. Before the LHC data, a band-shaped region of $m_A \simeq m_{H^\pm}$ is allowed in the $(m_{H^\pm}, m_A)$ space. For Type II, there exist a lower bound on $m_{H^\pm}$, which is constrained by the flavor data, and a lower bound on m_A due to the $\Delta\rho$. There are no upper bounds on m_A and $m_{H^\pm}$ at this stage. Large masses up to 10 TeV are possible, which are dominantly from the m_{12}^2 terms in Eq. (3). The degeneracy of $m_A \approx m_{H^\pm}$ is also explained by the same m_{12}^2 terms of m_A and $m_{H^\pm}$, which suppresses the new contribution to the $\Delta\rho$.

When the LHC Higgs data are applied, most of the green band region is excluded, leaving a very limited parameter space. As shown in the magnified small mass region, the LHC Higgs data put upper bounds on m_A and $m_{H^\pm}$. Both should be less than about 600 GeV. The strongest bound is from

---

[2]Our definition has additional factor of $\text{Br}(H^0 \to ii)/\text{Br}(h_{\text{SM}} \to ii)$ compared with the μ^{FD} in Ref. [36], which is the ratio of the FD production to direct production in the 2HDM.
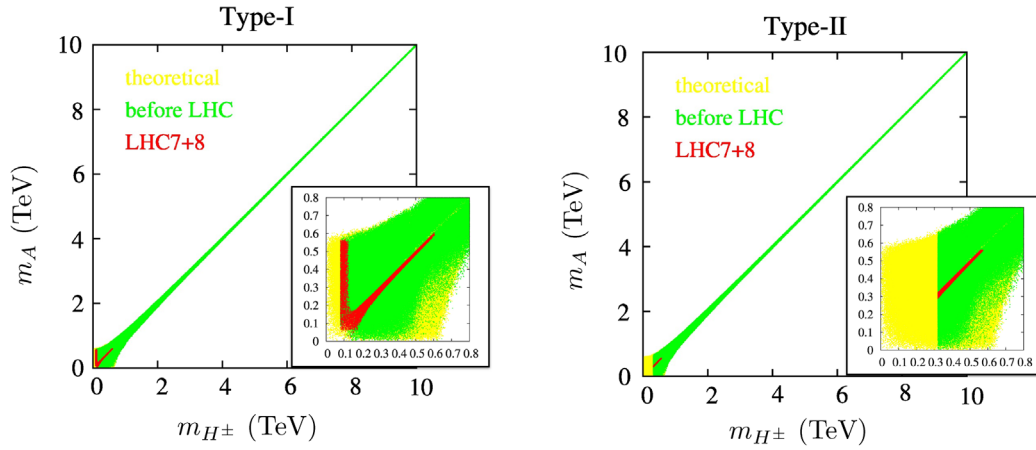
FIG. 1 (color online).   Constraints in the m_A versus $m_{H^\pm}$ plane for Type I and Type II 2HDM. Yellow points satisfy theoretical bounds. Green points satisfy up to the pre-LHC constraints while red points satisfy up to LHC constraints. The details of the constraints are summarized in Table I.

the observed mass of the 125 GeV state with high precision in Eq. (16). We expect that at the LHC Run 2 both A^0 and $H^\pm$ are to be probed in most of parameter space.

(iii) *Strong constraints from the* LHC *heavy Higgs data in Type* II: The 8 TeV LHC heavy Higgs searches in the decay channels of $\gamma\gamma$, $\tau^+\tau^-$, Z^0Z^0, and W^+W^- start to constrain the 2HDM [88]. We find that especially Type II is very sensitive to the results and thus does not allow too large t_β. In Fig. 2, we present the allowed parameters by the LHC Higgs data in the plane (m_A, t_β) for Type II. The heavy Higgs search results remove two regions, small t_β region with $m_A \lesssim 2m_t$ and large t_β region.

The small t_β region is excluded by the $\gamma\gamma$ channel through the gluon fusion production, similarly to the $h^0 = h_{125}$ case [60]. Both g-g-A^0 and γ-γ-A^0 vertices are loop induced, mainly through the top quark loop. Since all of four types have top quark Yukawa
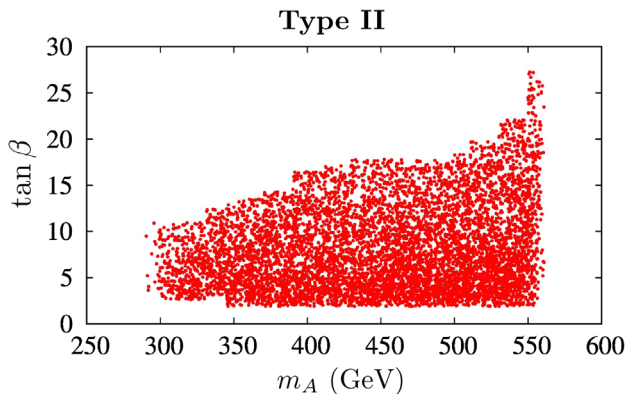

FIG. 2 (color online).   Allowed parameters by the LHC Higgs data in the plane (m_A, t_β) for Type II.

couplings with A^0 be inversely proportional to t_β, small t_β yields sizable gluon fusion production as well as sizable branching ratio into $\gamma\gamma$. If $m_A = 330$ GeV, for example, t_β should be above 2.5. This is stronger than the constraints from $b \to s\gamma$ and ΔM_{B_d} on small t_β like $t_\beta \gtrsim 1$ although the FCNC bound depends on the charged Higgs boson mass. Note that the exclusion of this small t_β region is common for all four types. As m_A goes beyond the $t\bar{t}$ threshold, the main decay mode of A^0 is into $t\bar{t}$, with the branching ratio practically one unless t_β is too large.

In Type II, large t_β region is excluded mainly by $b\bar{b} \to A^0 \to \tau^+\tau^-$ [88]. Here, both b quark and τ Yukawa couplings with A^0 are proportional to t_β, yielding the signal rate proportional to t_β^4. A large portion of the parameter space is excluded. For example, the $m_A = 300$ GeV case excludes $t_\beta \gtrsim 10$. In Type X and Type Y, the multiplication of τ and b quark Yukawa couplings with A^0 does not have t_β dependence. The LHC8 $b\bar{b} \to A^0 \to \tau^+\tau^-$ constraint for Types X and Y is not strong yet. In Type I, all of the Yukawa couplings are suppressed by t_β, which is weakly constrained.

(iv) *Preferring the alignment limit*: The deviation from the alignment limit is well parametrized by $s_{\beta-\alpha}$. In Fig. 3, we show the allowed parameter space in the $(s_{\beta-\alpha}, t_\beta)$ plane for Type I, II, X, and Y. Type I allows sizable deviation: $|s_{\beta-\alpha}| \lesssim 0.5$ in most cases, but even $|s_{\beta-\alpha}| \simeq 0.7$ is allowed scarcely. This is expected from the normalized Yukawa couplings in Eq. (10) which have the t_β-suppressed deviation from the alignment. The constraint from the LHC Higgs data on $s_{\beta-\alpha}$ is relatively weak. For other types, the t_β-enhanced Yukawa couplings constrain
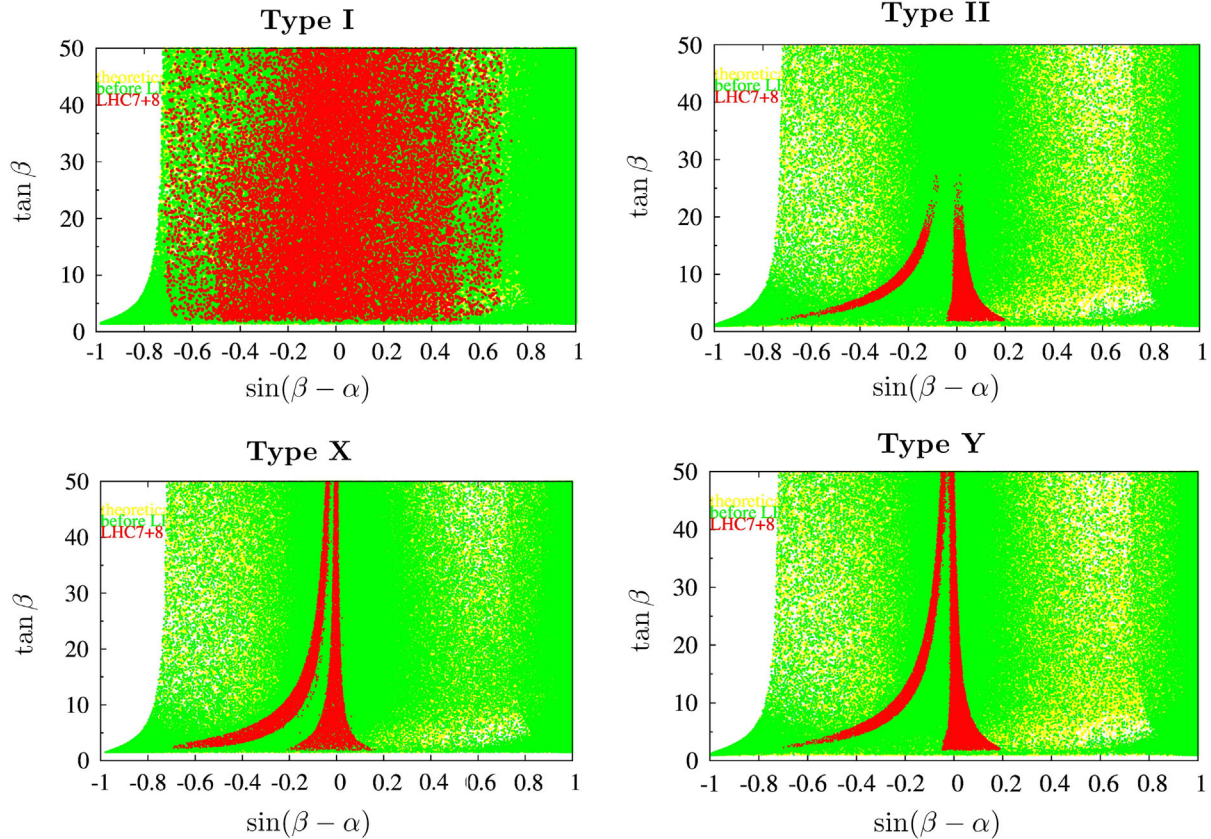
FIG. 3 (color online).   Constraints in the $(\sin(\beta-\alpha), \tan\beta)$ plane for Type I, II, X, and Y. Color scheme is the same as in Fig. 1.

the model, resulting in the preference to the alignment limit, stronger for large t_β.

For Type II, X, and Y, there are two separate regions of allowed parameters. One region is along the alignment line ($s_{\beta-\alpha}=0$). For small t_β which weakens the t_β-enhanced deviations in Eq. (10), $s_{\beta-\alpha}$ can be as large as 0.2. The other type of the allowed regions is a bit apart from the $s_{\beta-\alpha}=0$ line but toward negative $s_{\beta-\alpha}$. For small t_β, $s_{\beta-\alpha}$ can be as

FIG. 4 (color online).   Constraints in the (m_{12}^2, m_h) plane for Type I. Color scheme is the same as in Fig. 1.

large as -0.6. As shown in Fig. 2, Type II does not have the allowed region for $t_\beta > 20$ for the most part.

(v) *Low scale for* m_{12}^2: The m_{12}^2 term in the Higgs potential breaks the Z_2 symmetry softly. The explicit soft Z_2 breaking is to be understood as the result of spontaneous symmetry breaking in a more fundamental theory. Without a knowledge of the origin and dynamics of the Z_2 breaking, there is no guideline about the m_{12}^2 scale. In the hidden light Higgs scenario, however, the condition of $m_H = 125$ GeV constrains the m_{12}^2 scale very strongly. It is clearly shown in Fig. 4 by the allowed parameters in the (m_{12}^2, m_h) plane for Type I. Before the LHC data, m_{12}^2 is not limited, while the LEP bounds exclude most of the parameter space for $m_h < 114$ GeV. The current LHC Higgs data (red points) do prefer the low scale of m_{12}^2, which implies that the Z_2 parity is a good approximate symmetry in the scenario.
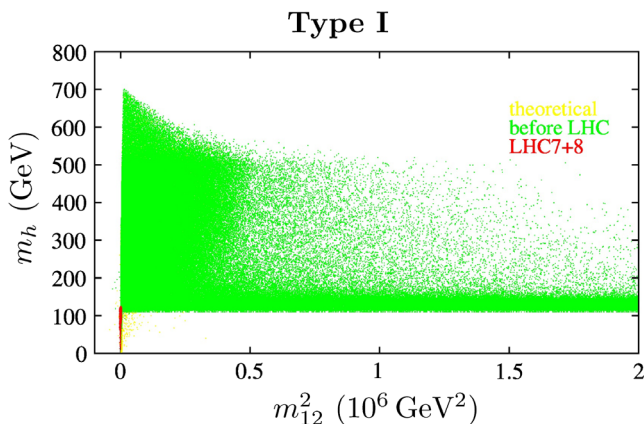
In Fig. 5, we show the constraints in the (m_{12}^2, m_h) plane for Type I, II, X, and Y, focused on the LHC allowed regions. All of the four types show similar shapes of the allowed regions: one exception is Type II where the allowed space is much smaller. As discussed before, this is because of the strong constraint from the heavy Higgs boson search in
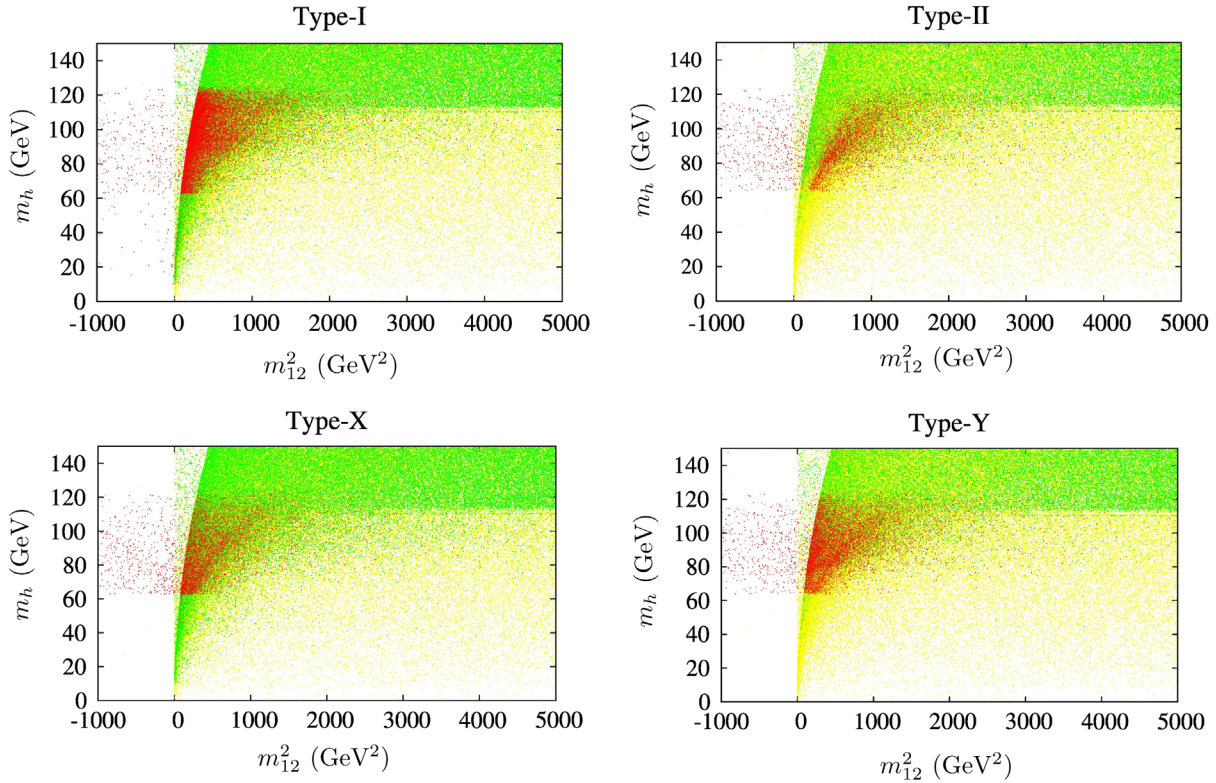
FIG. 5 (color online).   Constraints in the (m_{12}^2, m_h) plane for Type I and Type II. Color scheme is the same as in Fig. 1.

the b quark associated production followed by the decay into $\tau^+\tau^-$. Positive m_{12}^2 is preferred, although small negative value is also allowed. The magnitude of $|m_{12}|$ is below about 45 GeV mostly.

Note that very light h^0 is possible in Type I. However, too light scalar bosons may cause dangerous decay models such as $\eta \to \pi h^0$, $\Upsilon \to A^0\gamma$, and $J/\Psi \to A^0\gamma$. Although very light scalar bosons with mass below 10 GeV are not excluded in some parameter space [89–91], we require for both h^0 and A^0 to be heavier than 10 GeV for simplicity. Another important constraint is from the $H^0 \to h^0h^0$ decay, which affects the LHC Higgs signal strength measurement. In the alignment limit, the H^0-h^0-h^0 vertex, normalized by the SM vertex $g_{hhh}^{\rm SM} = 3m_{h_{\rm SM}}^2/v$, is

$$\hat{g}_{Hhh} = \frac{1}{3}\left[1 + 2\frac{m_h^2}{m_H^2} - 2\left(t_\beta + \frac{1}{t_\beta}\right)\frac{m_{12}^2}{m_H^2}\right] + \mathcal{O}(s_{\beta-\alpha}).$$

(20)

In the alignment limit, the decay $H^0 \to h^0h^0$ is sizable in general. In Types II, X, and Y where the alignment limit is strongly preferred (see Fig. 3), $\hat{g}_{Hhh}$ is too large to accommodate the LHC Higgs data unless m_{12}^2 and t_β are tuned to suppress $\hat{g}_{Hhh}$. It

turns out that the LHC Higgs data prefer $m_h > m_H/2$ in Type II, X, and Y in a general analysis based on the random generation of parameter points. On the other hand, a very light Higgs boson with $m_h < m_H/2$ is allowed, though less probable, when we carry out the analysis by choosing the special parameter choices leading to small enough $\hat{g}_{Hhh}$ as shown in Ref. [31].

(vi) *Strong bound on λ_2 but weak bounds on $\lambda_{1,3,4,5}$:* Figure 6 shows how much the current LHC Higgs data constrain the Higgs potential parameters λ_i's. For all of four types, λ_2 is almost determined to be around 0.26. This is mainly by the mass measurement of $m_H = 125$ GeV. Since m_{12}^2 is small (see Fig. 5) and $t_\beta > 1$ from the FCNC constraints, we have $m_H \sim \sqrt{\lambda_2}v$ in the large t_β limit: see Eqs. (5) and (6). The condition of $m_H = 125$ GeV almost fixes λ_2. Second, $\lambda_{345}(\equiv\lambda_3 + \lambda_4 + \lambda_5)$ is also limited by the observed Higgs boson mass in Types II, X, and Y. The other λ_i's are not seriously constrained. Compared to the pre-LHC (green) situation, the LHC Higgs data reduce the value of $\lambda_{1,3,4,5}$ by about half. Considering the role of the current LHC Higgs signal strength measurement in determining λ_2, we anticipate that the values of λ_i would be substantially reduced if additional Higgs bosons are observed.
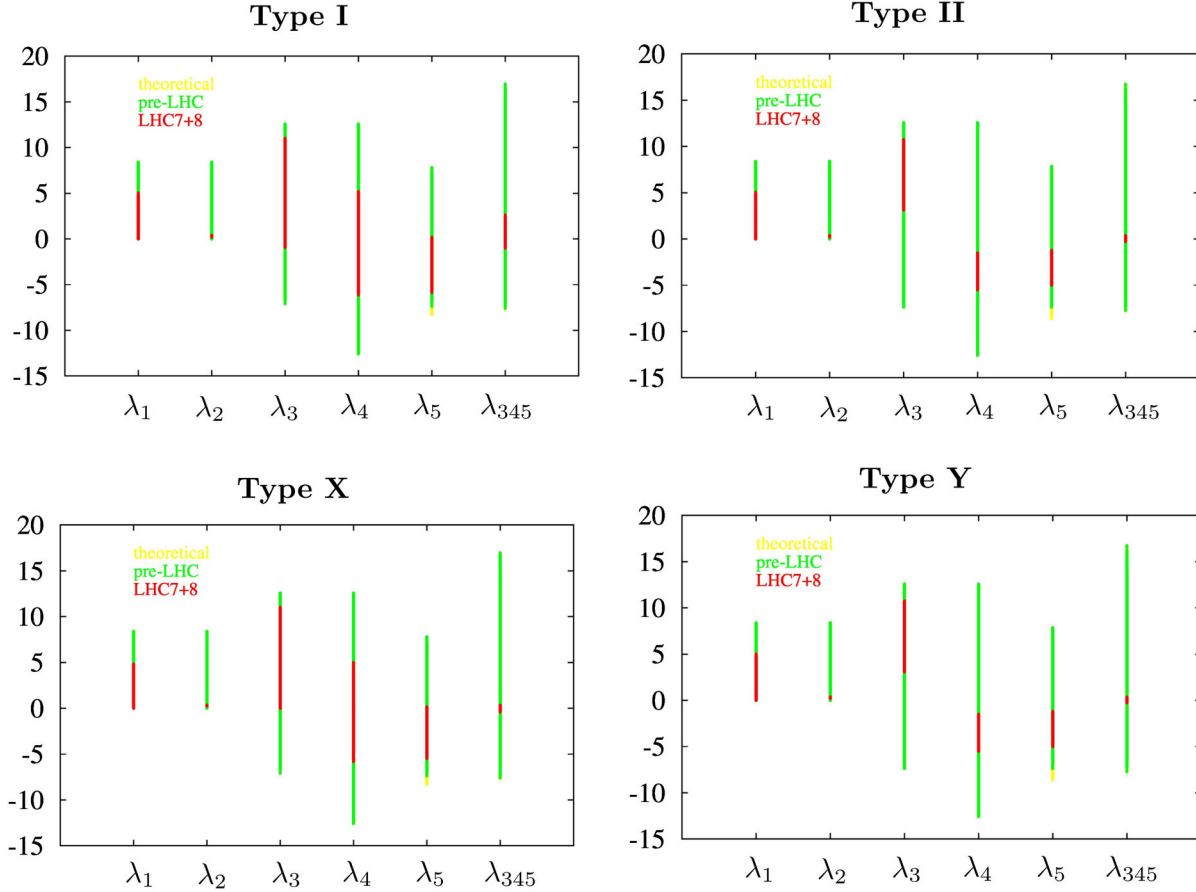
FIG. 6 (color online).   Constraints on $\lambda_{1,2,3,4,5}$ and $\lambda_{345} = \lambda_3 + \lambda_4 + \lambda_5$ for Type I, II, X, and Y. Color scheme is the same as in Fig. 1.

V. FUTURE PROSPECT OF $e^+e^- \rightarrow Z^0 H^0 H^0$

Focusing on the determination of the Higgs potential in the hidden light Higgs scenario, we study the current status of the Higgs triple and quartic couplings. First we study the allowed range of various Higgs triple couplings. In the normal setup with $h_{125} = h^0$, Ref. [92] showed that the LHC Higgs data constrain the normalized Higgs triple couplings $\hat{g}_{hhh}$ lies between 0.56 and 1 at 95% C.L. level in Type II. The Higgs boson pair production at a 14 TeV LHC was calculated for some benchmarks, not for the whole allowed parameter space, since the physical properties of the heavy Higgs bosons are weakly constrained in the normal setup. In the hidden light Higgs scenario, the heavy Higgs boson properties are shown to be significantly limited, which may result in higher predictability in the process involving the Higgs triple couplings.

In Fig. 7, we present the allowed values of the normalized Higgs triple couplings, $\hat{g}_{\phi_i \phi_j \phi_k}$ for $\phi_i = h^0$, H^0, A^0, $H^\pm$. For all of four types, the triple coupling involving two 125 GeV states, $\hat{g}_{hHH}$ and $\hat{g}_{HHH}$, are quite strongly constrained. Compared to the pre-LHC constraint, the LHC data restrict $\hat{g}_{hHH}$ and $\hat{g}_{HHH}$ within a few percent. In particular, $\hat{g}_{HHH}$ in Types II, X, and Y are very limited

between 0.69 and 1.1. In Type I that allows much larger parameter space, the reduction is into 10% level.

The quartic Higgs couplings are in general less constrained even in the hidden light Higgs scenario. In Fig. 8, we show the normalized quartic couplings by the SM value, with the three step constraints imposed. It is remarkable that $\hat{g}_{HHHH}$ and $\hat{g}_{hHHH}$ in Types II, X, and Y are quite significantly constrained as to be similar to the SM value. On the contrary, Type I does not have limited value of $\hat{g}_{HHHH}$ and $\hat{g}_{hHHH}$ because of the large allowed parameter space. Other quartic Higgs couplings can be very large compared with the SM value. Contrary to the SM case where the quartic coupling will remain unaccessible due to the tiny cross section of $e^+e^- \rightarrow Z^0 h_{SM} h_{SM} h_{SM}$ [11,12], some large quartic couplings can yield large enough cross section. In all of the four types, $\hat{g}_{hhhh}$ and $\hat{g}_{AAAA}$ can have the enhancement factor more than ten, which can be probed, e.g., through $e^+e^- \rightarrow Z^0 h^0 h^0 h^0$ and $\gamma\gamma \rightarrow A^0 A^0 A^0$, respectively.

In order to probe $\hat{g}_{hHH}$ and $\hat{g}_{HHH}$, we study the double Higgs-strahlung at an e^+e^- collider, $e^+e^- \rightarrow Z^0 H^0 H^0$ [93–95]. The Feynman diagrams are presented in Fig. 9. Since the physical properties of H^0 are well known, the
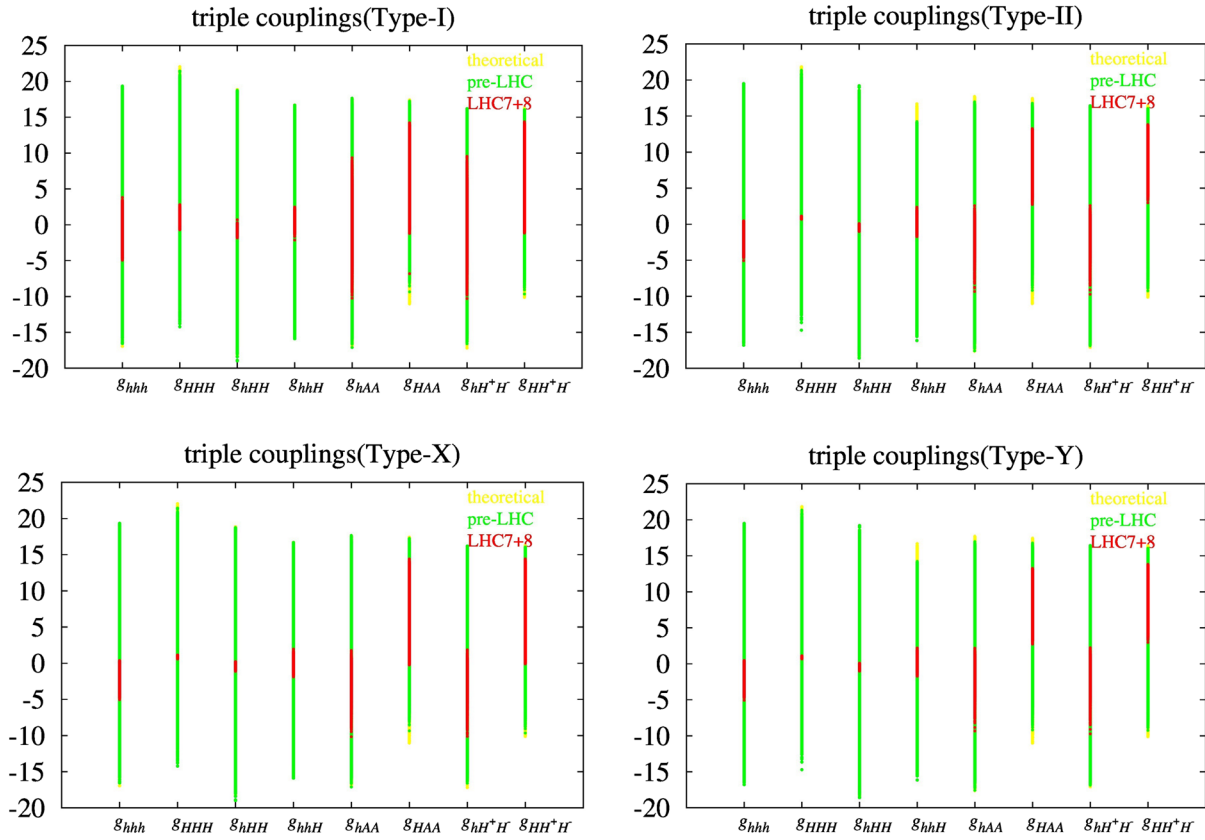
FIG. 7 (color online).   Constraints on $\hat{g}_{\phi_i \phi_j \phi_k}$ for Type I, II, X, and Y. Color scheme is the same as in Fig. 1.
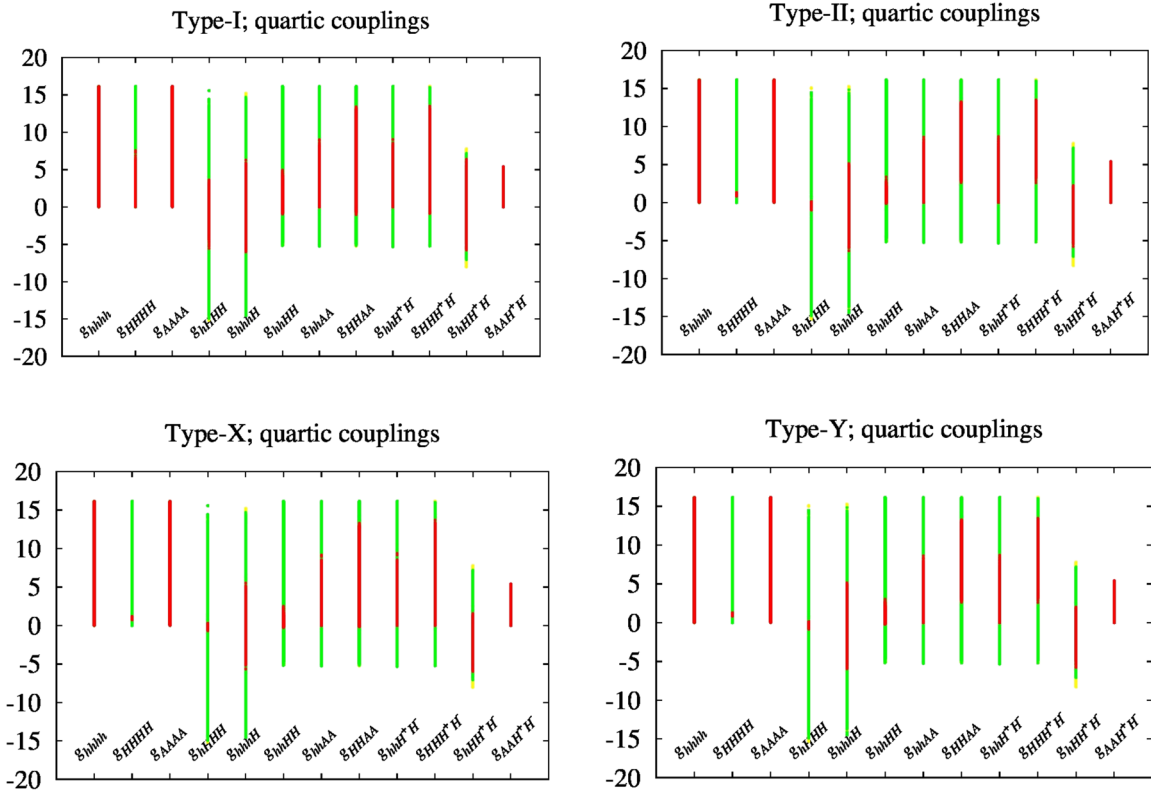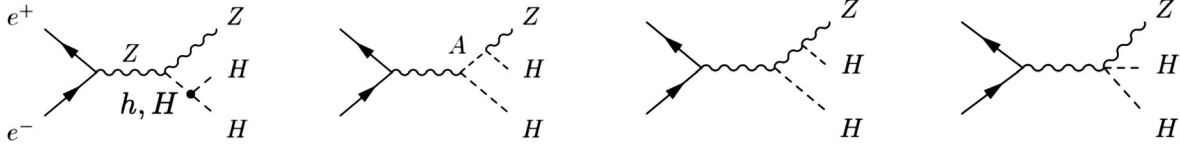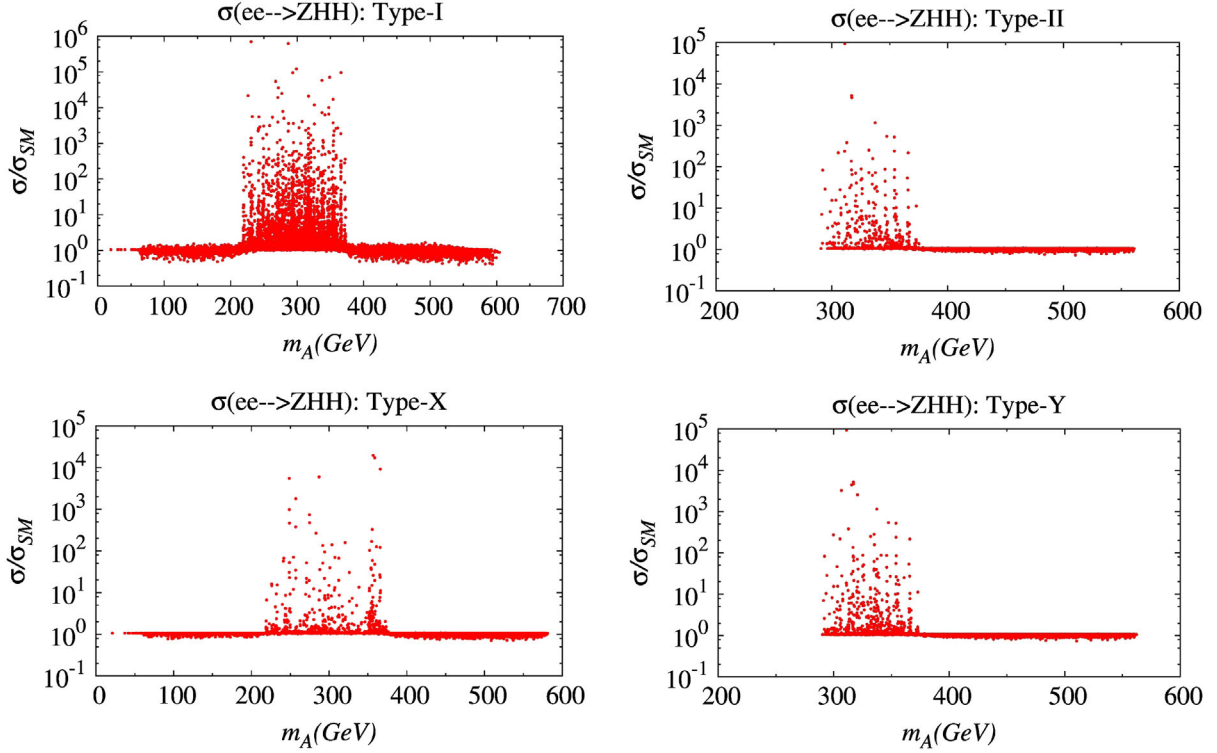

FIG. 8 (color online).   Constraints on $\hat{g}_{\phi_i \phi_j \phi_k \phi_\ell}$ for Type I, II, X, and Y. Color scheme is the same as in Fig. 1.

FIG. 9.   Feynman diagrams for $e^+e^- \to Z^0 H^0 H^0$.

FIG. 10 (color online).   The cross section of $e^+e^- \to Z^0 H^0 H^0$ versus m_A at $\sqrt{s} = 500$ GeV, normalized by the SM cross section, for the parameter points satisfying the LHC Higgs data.

Higgs boson can be used as a tagging particle for a new physics model. $\hat{g}_{hHH}$ and $\hat{g}_{HHH}$ contribute in the first diagram. The second Feynman diagram shows that the Z^0-H^0-A^0 vertex also contributes. As classified in Eq. (9), the Z^0-H^0-A^0 vertex is proportional to $s_{\beta-\alpha}$, which is suppressed in the alignment limit. If $s_{\beta-\alpha} \neq 0$ and the kinematical space includes the pole of the A^0 propagator, the total cross section can be highly enhanced.

   Figure 10 shows the expected total cross section of $e^+e^- \to Z^0 H^0 H^0$ versus m_A at $\sqrt{s} = 500$ GeV, normalized by the SM cross section. We accept only the parameter points which satisfy all of the current constraints. The analytic expression for $\sigma(e^+e^- \to Z^0 H^0 H^0)$ is referred to Ref. [95]. In most parameter space, the cross section in the 2HDM is very similar to that in the SM. In some parameter space, however, all of the four types allow highly enhanced cross section. The rate of increase can be as large as a factor of 10^4. As clearly shown in Types I and X, the enhancement occurs when $m_A \geq m_Z + m_H$.

VI. CONCLUSIONS

   We have investigated the meaning of the LHC Run 1 in the context of the hidden light Higgs scenario in the 2HDM with *CP* invariance and the softly broken Z_2 symmetry. We found that the LHC Run 1 data combined with other current constraints do not exclude the possibility that the observed scalar particle is the heavier *CP*-even Higgs boson H^0. The lighter *CP*-even Higgs boson h^0 is buried in the region of $\lesssim 120$ GeV. A remarkable consequence is that in order to make $m_H = 125$ GeV the Z_2 symmetry breaking parameter m_{12}^2 cannot be large, which renders $m_{A,H^\pm}$ rather light at the sub-TeV scale. We found the upper bounds on $m_{A,H^\pm}$ to be around 600 GeV. Since the mass scales of other Higgs bosons are not far from the LHC reach, the hidden light Higgs scenario can be tested in the near future.

   We also found that the LHC Run 1 data begin to constrain the Higgs potential of the 2HDM. In particular, the values of λ_2 and $\hat{g}_{HHH}$ are almost determined. The cross section of $e^+e^- \to Z^0 H^0 H^0$ is expected to be close to that of the SM, while in a limited region of m_A around 300 GeV

it could be highly enhanced. The Higgs quartic couplings are less constrained. Hopefully future lepton colliders could check our predictions.

ACKNOWLEDGMENTS

[1] G. Aad *et al.* (ATLAS Collaboration), Observation of a new particle in the search for the Standard Model Higgs boson with the ATLAS detector at the LHC, Phys. Lett. B **716**, 1 (2012); S. Chatrchyan *et al.* (CMS Collaboration), Observation of a new boson at a mass of 125 GeV with the CMS experiment at the LHC, Phys. Lett. B **716**, 30 (2012).

[2] CMS Collaboration, Report No. CMS-PAS-HIG-14-009; G. Aad *et al.* (ATLAS Collaboration), Measurement of the Higgs boson mass from the $H \to \gamma\gamma$ and $H \to ZZ^* \to 4\ell$ channels with the ATLAS detector using 25 fb^{-1} of pp collision data, Phys. Rev. D **90**, 052004 (2014).

[3] G. Aad *et al.* (ATLAS Collaboration), Measurement of Higgs boson production in the diphoton decay channel in pp collisions at center-of-mass energies of 7 and 8 TeV with the ATLAS detector, Phys. Rev. D **90**, 112015 (2014).

[4] G. Aad *et al.* (ATLAS Collaboration), Search for $H \to \gamma\gamma$ produced in association with top quarks and constraints on the Yukawa coupling between the top quark and the Higgs boson using data taken at 7 TeV and 8 TeV with the ATLAS detector, Phys. Lett. B **740**, 222 (2015).

[5] V. Khachatryan *et al.* (CMS Collaboration), Observation of the diphoton decay of the Higgs boson and measurement of its properties, Eur. Phys. J. C **74**, 3076 (2014).

[6] H. S. Cheon and S. K. Kang, Constraining parameter space in type-II two-Higgs doublet model in light of a 126 GeV Higgs boson, J. High Energy Phys. 09 (2013) 085; S. Chang, S. K. Kang, J. P. Lee, K. Y. Lee, S. C. Park, and J. Song, Comprehensive study of two Higgs doublet model in light of the new boson with mass around 125 GeV, J. High Energy Phys. 05 (2013) 075; N. Chakrabarty, U. K. Dey, and B. Mukhopadhyaya, High-scale validity of a two-Higgs doublet scenario: A study including LHC data, J. High Energy Phys. 12 (2014) 166.

[7] S. Chang, S. K. Kang, J. P. Lee, K. Y. Lee, S. C. Park, and J. Song, Two Higgs doublet models for the LHC Higgs boson data at $\sqrt{s} = 7$ and 8 TeV, J. High Energy Phys. 09 (2014) 101.

[8] J. F. Gunion and H. E. Haber, The *CP* conserving two Higgs doublet model: The approach to the decoupling limit, Phys. Rev. D **67**, 075019 (2003).

[9] A. Noble and M. Perelstein, Higgs self-coupling as a probe of electroweak phase transition, Phys. Rev. D **78**, 063518 (2008).

[10] A. Katz and M. Perelstein, Higgs couplings and electroweak phase transition, J. High Energy Phys. 07 (2014) 108.

[11] M. Battaglia, E. Boos, and W. M. Yao, Studying the Higgs potential at the e+ e− linear collider, eConf C010630, E3016 (2001).

[12] M. Beyer, W. Kilian, P. Krstonosic, K. Monig, J. Reuter, E. Schmidt, and H. Schroder, Determination of new electroweak parameters at the ILC—Sensitivity to new physics, Eur. Phys. J. C **48**, 353 (2006).

[13] J. F. Gunion and H. E. Haber, The *CP* conserving two Higgs doublet model: The approach to the decoupling limit, Phys. Rev. D **67**, 075019 (2003); G. C. Branco, P. M. Ferreira, L. Lavoura, M. N. Rebelo, M. Sher, and J. P. Silva, Theory and phenomenology of two-Higgs-doublet models, Phys. Rep. **516**, 1 (2012).

[14] S. L. Glashow and S. Weinberg, Natural conservation laws for neutral currents, Phys. Rev. D **15**, 1958 (1977); E. A. Paschos, Diagonal neutral currents, Phys. Rev. D **15**, 1966 (1977).

[15] M. Aoki, S. Kanemura, K. Tsumura, and K. Yagyu, Models of Yukawa interaction in the two Higgs doublet model, and their collider phenomenology, Phys. Rev. D **80**, 015017 (2009).

[16] A. G. Akeroyd, Nonminimal neutral Higgs bosons at LEP-2, Phys. Lett. B **377**, 95 (1996).

[17] C. Y. Chen and S. Dawson, Exploring two Higgs doublet models through Higgs production, Phys. Rev. D **87**, 055016 (2013).

[18] C. W. Chiang and K. Yagyu, Implications of Higgs boson search data on the two-Higgs doublet models with a softly broken Z_2 symmetry, J. High Energy Phys. 07 (2013) 160.

[19] B. Grinstein and P. Uttayarat, Carving out parameter space in Type-II two Higgs doublets model, J. High Energy Phys. 06 (2013) 094.

[20] O. Eberhardt, U. Nierste, and M. Wiebusch, Status of the two-Higgs-doublet model of type II, J. High Energy Phys. 07 (2013) 118.

[21] G. Belanger, B. Dumont, U. Ellwanger, J. F. Gunion, and S. Kraml, Global fit to Higgs signal strengths and couplings and implications for extended Higgs sectors, Phys. Rev. D **88**, 075008 (2013).

[22] K. Cheung, J. S. Lee, and P. Y. Tseng, Higgcision in the two-Higgs doublet models, J. High Energy Phys. 01 (2014) 085.

[23] A. Celis, V. Ilisie, and A. Pich, Towards a general analysis of LHC data within two-Higgs-doublet models, J. High Energy Phys. 12 (2013) 095.

[24] L. Wang and X. F. Han, Status of the aligned two-Higgs-doublet model confronted with the Higgs data, J. High Energy Phys. 04 (2014) 128.

[25] S. Kanemura, K. Tsumura, K. Yagyu, and H. Yokoya, Fingerprinting nonminimal Higgs sectors, Phys. Rev. D **90**, 075001 (2014).

[26] P. M. Ferreira, R. Guedes, J. F. Gunion, H. E. Haber, M. O. P. Sampaio, and R. Santos, The CP-conserving 2HDM after the 8 TeV run, arXiv:1407.4396.

[27] A. Broggio, E. J. Chun, M. Passera, K. M. Patel, and S. K. Vempati, Limiting two-Higgs-doublet models, J. High Energy Phys. 11 (2014) 058.

[28] D. Chowdhury and O. Eberhardt, Global fits of the two-loop renormalized Two-Higgs-Doublet model with soft Z_2 breaking, arXiv:1503.08216.

[29] L. Wang and X. F. Han, Study of the heavy *CP*-even Higgs with mass 125 GeV in two-Higgs-doublet models at the LHC and ILC, J. High Energy Phys. 11 (2014) 085.

[30] S. Kanemura, H. Yokoya, and Y. J. Zheng, Complementarity in direct searches for additional Higgs bosons at the LHC and the International Linear Collider, Nucl. Phys. **B886**, 524 (2014).

[31] J. Bernon, J. F. Gunion, Y. Jiang, and S. Kraml, Light Higgs bosons in two-Higgs-doublet models, Phys. Rev. D **91**, 075019 (2015).

[32] B. Coleppa, F. Kling, and S. Su, Constraining type II 2HDM in light of LHC Higgs searches, J. High Energy Phys. 01 (2014) 161.

[33] E. Cervero and J. M. Gerard, Minimal violation of flavour and custodial symmetries in a vectophobic two-Higgs-doublet-model, Phys. Lett. B **712**, 255 (2012).

[34] S. de Visscher, J. M. Gerard, M. Herquet, V. Lemaitre, and F. Maltoni, Unconventional phenomenology of a minimal two-Higgs-doublet model, J. High Energy Phys. 08 (2009) 042.

[35] P. M. Ferreira, R. Guedes, M. O. P. Sampaio, and R. Santos, Wrong sign and symmetric limits and non-decoupling in 2HDMs, J. High Energy Phys. 12 (2014) 067.

[36] B. Dumont, J. F. Gunion, Y. Jiang, and S. Kraml, Constraints on and future prospects for two-Higgs-doublet models in light of the LHC Higgs signal, Phys. Rev. D **90**, 035021 (2014).

[37] B. Bhattacherjee, A. Chakraborty, and A. Choudhury, Status of MSSM Higgs Sector using Global Analysis and Direct Search Bounds, and Future Prospects at the HL-LHC, arXiv:1504.04308.

[38] I. P. Ivanov, Minkowski space structure of the Higgs potential in 2HDM, Phys. Rev. D **75**, 035001 (2007); **76**, 039902(E) (2007).

[39] A. Arhrib, Unitarity constraints on scalar parameters of the Standard and Two Higgs Doublets Model, arXiv:hep-ph/0012353.

[40] G. C. Branco, P. M. Ferreira, L. Lavoura, M. N. Rebelo, M. Sher, and J. P. Silva, Theory and phenomenology of two-Higgs-doublet models, Phys. Rep. **516**, 1 (2012).

[41] A. Sopczak, Higgs Physics: from LEP to a Future Linear Collider, arXiv:hep-ph/0502002.

[42] R. Barate *et al.* (LEP Working Group for Higgs boson searches and ALEPH and DELPHI and L3 and OPAL Collaborations), Search for the standard model Higgs boson at LEP, Phys. Lett. B **565**, 61 (2003); S. Schael *et al.* (ALEPH and DELPHI and L3 and OPAL and LEP Working Group for Higgs Boson Searches Collaborations), Search for neutral MSSM Higgs bosons at LEP, Eur. Phys. J. C **47**, 547 (2006).

[43] K. A. Olive *et al.* (Particle Data Group Collaboration), Review of particle physics (RPP), Chin. Phys. C **38**, 090001 (2014).

[44] J. F. Gunion, H. E. Haber, G. Kane, and S. Dawson, *The Higgs Hunter's Guide* (Addison-Wesley Publishing Company, Reading, MA, 1990).

[45] P. H. Chankowski, M. Krawczyk, and J. Zochowski, Implications of the precision data for very light Higgs boson scenario in 2HDM(II), Eur. Phys. J. C **11**, 661 (1999).

[46] W. S. Hou and R. S. Willey, Effects of charged Higgs bosons on the processes $b \to s\Gamma$, $b \to sg*$ and $b \to s$ Lepton $+$ Lepton$-$, Phys. Lett. B **202**, 591 (1988); B. Grinstein and M. B. Wise, Weak radiative B meson decay as a probe of the Higgs sector, Phys. Lett. B **201**, 274 (1988); B. Grinstein, R. P. Springer, and M. B. Wise, Strong interaction effects in weak radiative $\bar{B}$ meson decay, Nucl. Phys. **B339**, 269 (1990); V. D. Barger, J. L. Hewett, and R. J. N. Phillips, New constraints on the charged Higgs sector in two Higgs doublet models, Phys. Rev. D **41**, 3421 (1990); S. Bertolini, F. Borzumati, A. Masiero, and G. Ridolfi, Effects of supergravity induced electroweak breaking on rare *B* decays and mixings, Nucl. Phys. **B353**, 591 (1991).

[47] F. Mahmoudi and O. Stal, Flavor constraints on the two-Higgs-doublet model with general Yukawa couplings, Phys. Rev. D **81**, 035016 (2010).

[48] A. Abulencia *et al.* (CDF Collaboration), Search for Charged Higgs Bosons from Top Quark Decays in $p\bar{p}$ Collisions at $\sqrt{s} = 1.96$-TeV., Phys. Rev. Lett. **96**, 042003 (2006); V. M. Abazov *et al.* (D0 Collaboration), Direct Search for Charged Higgs Bosons in Decays of Top Quarks, Phys. Rev. Lett. **88**, 151803 (2002).

[49] G. Aad *et al.* (ATLAS Collaboration), Search for charged Higgs bosons decaying via $H^{\pm} \to \tau^{\pm}\nu$ in fully hadronic final states using pp collision data at $\sqrt{s} = 8$ TeV with the ATLAS detector, J. High Energy Phys. 03 (2015) 088; The ATLAS collaboration, Reports No. ATLAS-CONF-2013-090, No. ATLAS-COM-CONF-2013-107.

[50] CMS Collaboration, Report No. CMS-PAS-HIG-14-020; S. Chatrchyan *et al.* (CMS Collaboration), Search for a light charged Higgs boson in top quark decays in pp collisions at $\sqrt{s} = 7$ TeV, J. High Energy Phys. 07 (2012) 143.

[51] CMS Collaboration, Report No. CMS-PAS-HIG-13-035.

[52] G. Aad *et al.* (ATLAS Collaboration), Search for Scalar Diphoton Resonances in the Mass Range 65–600 GeV with the ATLAS Detector in pp Collision Data at $\sqrt{s} = 8$ TeV, Phys. Rev. Lett. **113**, 171801 (2014).

[53] CMS Collaboration, Report No. CMS-PAS-HIG-14-006.

[54] G. Aad *et al.* (ATLAS Collaboration), Search for neutral Higgs bosons of the minimal supersymmetric standard model in pp collisions at $\sqrt{s} = 8$ TeV with the ATLAS detector, J. High Energy Phys. 11 (2014) 056.

[55] V. Khachatryan *et al.* (CMS Collaboration), Search for neutral MSSM Higgs bosons decaying to a pair of tau leptons in pp collisions, J. High Energy Phys. 10 (2014) 160.

[56] A. Arhrib, P. M. Ferreira, and R. Santos, Are there hidden scalars in LHC Higgs results?, J. High Energy Phys. 03 (2014) 053.

[57] N. Craig, J. Galloway, and S. Thomas, Searching for Signs of the Second Higgs Doublet, arXiv:1305.2424; A. Celis, V. Ilisie, and A. Pich, Towards a general analysis of LHC data

within two-Higgs-doublet models, J. High Energy Phys. 12 (2013) 095; Status of the aligned two-Higgs-doublet model confronted with the Higgs data, J. High Energy Phys. 04 (2014) 128; P. S. B. Dev and A. Pilaftsis, Maximally symmetric two Higgs doublet model with natural standard model alignment, J. High Energy Phys. 12 (2014) 024.

[58] A. Barroso, P. M. Ferreira, I. P. Ivanov, and R. Santos, Metastability bounds on the two Higgs doublet model, J. High Energy Phys. 06 (2013) 045.

[59] J.-M. Gerard and M. Herquet, A Twisted Custodial Symmetry in the Two-Higgs-Doublet Model, Phys. Rev. Lett. **98,** 251802 (2007).

[60] J. Song and Y. W. Yoon, Gigantic diphoton rate of heavy Higgs bosons in the aligned two Higgs doublet models with small tan, Phys. Rev. D **91,** 113012 (2015).

[61] E. Barberio et al. (Heavy Flavor Averaging Group Collaboration), Averages of b-hadron and c-hadron Properties at the End of 2007, arXiv:0808.1297.

[62] M. Jung, A. Pich, and P. Tuzon, Charged-Higgs phenomenology in the aligned two-Higgs-doublet model, J. High Energy Phys. 11 (2010) 003.

[63] S. Schael et al. (ALEPH and DELPHI and L3 and OPAL and SLD and LEP Electroweak Working Group and SLD Electroweak Group and SLD Heavy Flavour Group Collaborations), Precision electroweak measurements on the Z resonance, Phys. Rep. **427,** 257 (2006).

[64] J. Bernabeu, A. Pich, and A. Santamaria, Top quark mass from radiative corrections to the $Z \rightarrow b$ anti-b decay, Nucl. Phys. **B363,** 326 (1991); H. E. Haber and H. E. Logan, Radiative corrections to the Z b anti-b vertex and constraints on extended Higgs sectors, Phys. Rev. D **62,** 015011 (2000); G. Degrassi and P. Slavich, QCD corrections in two-Higgs-doublet extensions of the standard model with minimal flavor violation, Phys. Rev. D **81,** 075001 (2010).

[65] M. Baak and R. Kogler, The global electroweak Standard Model fit after the Higgs discovery, arXiv:1306.0571; H. Flacher, M. Goebel, J. Haller, A. Hocker, K. Monig, and J. Stelzer, Revisiting the global electroweak fit of the standard model and beyond with Gfitter, Eur. Phys. J. C **60,** 543 (2009); **71,** 1718(E) (2011).

[66] J. P. Lees et al. (BABAR Collaboration), Evidence for an Excess of $\bar{B} \rightarrow D^{(*)}\tau^{-}\bar{\nu}_{\tau}$ Decays, Phys. Rev. Lett. **109,** 101802 (2012).

[67] R. Aaij et al. (LHCb Collaboration), Measurement of the Ratio of Branching Fractions $\mathcal{B}(\bar{B}^{0} \rightarrow D^{*+}\tau^{-}\bar{\nu}_{\tau}))/\mathcal{B}(\bar{B}^{0} \rightarrow D^{*+}\mu^{-}\bar{\nu}_{\mu})$, Phys. Rev. Lett. **115,** 111803 (2015).

[68] M. Huschle et al. (Belle Collaboration), Measurement of the branching ratio of $\bar{B} \rightarrow D^{(*)}\tau^{-}\bar{\nu}_{\tau}$ relative to $\bar{B} \rightarrow D^{(*)}l^{-}\bar{\nu}_{l}$ decays with hadronic tagging at Belle, arXiv:1507.03233.

[69] G. Aad et al. (ATLAS Collaboration), Measurement of the Higgs boson mass from the $H \rightarrow \gamma\gamma$ and $H \rightarrow ZZ^{*} \rightarrow 4\ell$ channels with the ATLAS detector using 25 fb^{-1} of pp collision data, Phys. Rev. D **90,** 052004 (2014).

[70] V. Khachatryan et al. (CMS Collaboration), Precise determination of the mass of the Higgs boson and tests of compatibility of its couplings with the standard model predictions using proton collisions at 7 and 8 TeV, Eur. Phys. J. C **75,** 212 (2015).

[71] G. Aad et al. (ATLAS and CMS Collaborations), Combined Measurement of the Higgs Boson Mass in pp Collisions at $\sqrt{s} = 7$ and 8 TeV with the ATLAS and CMS Experiments, Phys. Rev. Lett. **114,** 191803 (2015).

[72] CMS Collaboration, Report No. CMS-PAS-HIG-13-026.

[73] P. Turner (CMS Collaboration), $\sqrt{s} = 8$ TeV Search for $t\bar{t}$ resonances in semileptonic final states in pp collisions at , arXiv:1310.7859; B. A. Gonzalez, Searches for vector-like quarks and $t\bar{t}$ resonances with the ATLAS detector, arXiv:1409.3340.

[74] S. Jung, J. Song, and Y. W. Yoon, Dip or nothingness of a Higgs resonance from the interference with a complex phase, Phys. Rev. D **92,** 055009 (2015).

[75] D. Dicus, A. Stange, and S. Willenbrock, Higgs decay to top quarks at hadron colliders, Phys. Lett. B **333,** 126 (1994).

[76] A. Djouadi, L. Maiani, A. Polosa, J. Quevillon, and V. Riquer, Fully covering the MSSM Higgs sector at the LHC, J. High Energy Phys. 06 (2015) 168.

[77] The ATLAS Collaboration, Reports No. ATLAS-CONF-2014-060, No. ATLAS-COM-CONF-2014-078.

[78] The ATLAS Collaboration, Reports No. ATLAS-CONF-2014-009, No. ATLAS-COM-CONF-2014-013.

[79] The ATLAS Collaboration, Reports No. ATLAS-CONF-2014-061, No. ATLAS-COM-CONF-2014-080.

[80] The ATLAS Collaboration, Report Nos. ATLAS-CONF-2014-011, ATLAS-COM-CONF-2014-004.

[81] M. M. Llacer (ATLAS Collaboration), Search for the Standard Model Higgs boson production in association with top quarks in pp collisions at 8 TeV with the ATLAS detector, arXiv:1411.7638.

[82] S. Chatrchyan et al. (CMS Collaboration), Measurement of Higgs boson production and properties in the WW decay channel with leptonic final states, J. High Energy Phys. 01 (2014) 096.

[83] S. Chatrchyan et al. (CMS Collaboration), Measurement of the properties of a Higgs boson in the four-lepton final state, Phys. Rev. D **89,** 092007 (2014).

[84] S. Chatrchyan et al. (CMS Collaboration), Evidence for the 125 GeV Higgs boson decaying to a pair of τ leptons, J. High Energy Phys. 05 (2014) 104.

[85] C. Vernieri (CMS Collaboration), Search for the Higgs boson in the $b\bar{b}$ decay channel using the CMS detector, arXiv:1411.4362.

[86] G. Aad et al. (ATLAS Collaboration), Search for the $b\bar{b}$ decay of the standard model Higgs boson in associated $(W/Z)H$ production with the ATLAS detector, J. High Energy Phys. 01 (2015) 069.

[87] S. Chatrchyan et al. (CMS Collaboration), Search for the standard model Higgs boson produced in association with a W or a Z boson and decaying to bottom quarks, Phys. Rev. D **89,** 012003 (2014).

[88] N. Craig, F. D'Eramo, P. Draper, S. Thomas, and H. Zhang, The hunt for the rest of the Higgs bosons, J. High Energy Phys. 06 (2015) 137.

[89] F. Larios, G. Tavares-Velasco, and C. P. Yuan, Update on a very light CP odd scalar in the two Higgs doublet model, Phys. Rev. D **66,** 075006 (2002).

[90] D. L. Anderson, C. D. Carone, and M. Sher, Probing the light pseudoscalar window, Phys. Rev. D **67**, 115013 (2003).

[91] J. D. Clarke, R. Foot, and R. R. Volkas, Phenomenology of a very light scalar (100 MeV $< m_h <$ 10 GeV) mixing with the SM Higgs, J. High Energy Phys. 02 (2014) 123.

[92] J. Baglio, O. Eberhardt, U. Nierste, and M. Wiebusch, Benchmarks for Higgs pair production and heavy Higgs boson searches in the two-Higgs-doublet model of Type II, Phys. Rev. D **90**, 015008 (2014).

[93] A. Djouadi, The anatomy of electro-weak symmetry breaking. II. The Higgs bosons in the minimal supersymmetric model, Phys. Rep. **459**, 1 (2008).

[94] W. Kilian, M. Kramer, and P. M. Zerwas, Higgsstrahlung and WW fusion in $e+ e-$ collisions, Phys. Lett. B **373**, 135 (1996).

[95] A. Djouadi, W. Kilian, M. Muhlleitner, and P. M. Zerwas, Testing Higgs self-couplings at $e+ e-$ linear colliders, Eur. Phys. J. C **10**, 27 (1999).